Pancreatic β-Cell Response to Increased Metabolic Demand and to Pharmacologic Secretagogues Requires EPAC2A

Woo-Jin Song,[1] Prosenjit Mondal,[1] Yuanyuan Li,[1] Suh Eun Lee,[1] and Mehboob A. Hussain[1,2,3]

Incretin hormone action on β-cells stimulates in parallel two different intracellular cyclic AMP-dependent signaling branches mediated by protein kinase A and exchange protein activated by cAMP islet/brain isoform 2A (EPAC2A). Both pathways contribute toward potentiation of glucose-stimulated insulin secretion (GSIS). However, the overall functional role of EPAC2A in β-cells as it relates to in vivo glucose homeostasis remains incompletely understood. Therefore, we have examined in vivo GSIS in global EPAC2A knockout mice. Additionally, we have conducted in vitro studies of GSIS and calcium dynamics in isolated EPAC2A-deficient islets. EPAC2A deficiency does not impact GSIS in mice under basal conditions. However, when mice are exposed to diet-induced insulin resistance, pharmacologic secretagogue stimulation of β-cells with an incretin hormone glucagon-like peptide-1 analog or with a fatty acid receptor 1/G protein–coupled receptor 40 selective activator, EPAC2A is required for the increased β-cell response to secretory demand. Under these circumstances, EPAC2A is required for potentiating the early dynamic increase in islet calcium levels after glucose stimulation, which is reflected in potentiated first-phase insulin secretion. These studies broaden our understanding of EPAC2A function and highlight its significance during increased secretory demand or drive on β-cells. Our findings advance the rationale for developing EPAC2A-selective pharmacologic activators for β-cell–targeted pharmacotherapy in type 2 diabetes. ***Diabetes*** **62:2796–2807, 2013**

Pancreatic β-cells secrete insulin by regulated exocytosis to tightly control glucose homeostasis. In conditions of increased metabolic demand on insulin action, such as obesity-related insulin resistance, β-cells are capable of increasing by several-fold glucose-stimulated insulin secretion (GSIS), thereby maintaining tight glycemic regulation (1). Failure of β-cells to adequately respond to increased metabolic demand on insulin secretion (β-cell dysfunction) results in diabetes (1,2).

GSIS is potentiated by activation of the incretin hormone glucagon-like peptide-1 receptor (GLP-1R), which is expressed at high density on pancreatic β-cells. GLP-1R activation potentiates GSIS when blood glucose surpasses a threshold of physiologic fasting glycemia. Pharmacologic activation of GLP-1R with the GLP-1 agonist exendin-4 (E4) can reverse pancreatic β-cell dysfunction in humans with type 2 diabetes mellitus (T2DM) and increases GSIS, leading to improved glycemic control while also avoiding hypoglycemia (3).

Ligand-induced GLP-1R activation stimulates intracellular cAMP synthesis, which in turn engages two distinct intracellular signaling pathways: protein kinase A (PKA) and the exchange protein activated by cAMP islet/brain isoform 2A (EPAC2A) (3). Selective disinhibition of PKA activity in murine β-cells greatly augments GSIS (4). Conversely, genetic EPAC2A ablation in mice has little effect on glucose homeostasis (5). However, in contrast to these in vivo observations, in vitro studies using pharmacologic GLP-1R activation and EPAC2A activation using EPAC2A-selective cAMP analogs (ESCA) suggest that upon a glucose stimulus to β-cells, EPAC2A is important for potentiating a rise in intracellular Ca^{2+} (iCa^{2+}) (6–8), a prerequisite for insulin vesicle exocytosis (9). In addition, EPAC2A is activated by cAMP levels that are significantly higher than those required to activate PKA (10,11). Furthermore, pharmacologic stimulation of β-cells with the sulfonylurea class of antidiabetic drugs activate EPAC2A in a cAMP-independent manner to stimulate insulin secretion (5).

Based on these considerations, we reasoned that EPAC2A function may be of general importance in β-cells, particularly during circumstances that demand increased insulin secretion either in response to insulin resistance or to pharmacologic stimuli. We therefore exposed EPAC2A-deficient mice and their isolated islets to a variety of conditions that provoke augmented β-cell insulin secretory response to glucose. Our findings indicate that EPAC2A is required for increased GSIS in the face of diet-induced insulin resistance, during pharmacologic stimulation with the GLP-1 analog E4, as well as during stimulation with a selective fatty acid receptor 1/G protein–coupled receptor 40 (GPR40) activator (12,13). In a genetic mouse model of β-cell autonomous GSIS potentiation, EPAC2A is required for achieving maximum insulin secretion. In all of these circumstances, EPAC2A is important for potentiating the initial increase in β-cell iCa^{2+} after glucose stimulation.

Our findings suggest that while under basal conditions, EPAC2A plays a minor role in regulating GSIS, EPAC2A function occupies an important role in augmenting GSIS under conditions of increased β-cell secretory activity. In particular, our studies suggest a role for EPAC2A in the adaptation of β-cell secretory response to insulin resistance. Our findings broaden the role of EPAC2A beyond its currently appreciated function in incretin hormone-stimulated cAMP signaling. These observations provide further rationale for developing EPAC2A-selective activators

From the [1]Department of Pediatrics, Johns Hopkins University, Baltimore, Maryland; the [2]Department of Medicine, Johns Hopkins University, Baltimore, Maryland; and the [3]Department of Biological Chemistry, Johns Hopkins University, Baltimore, Maryland.
Corresponding author: Mehboob A. Hussain, mhussai4@jhmi.edu.
Received 10 October 2012 and accepted 26 March 2013.
DOI: 10.2337/db12-1394
This article contains Supplementary Data online at http://diabetes.diabetesjournals.org/lookup/suppl/doi:10.2337/db12-1394/-/DC1.
W.-J.S. and P.M. contributed equally to this study.

See accompanying commentary, p. 2665.

for individually tailored pharmacotherapy in humans with β-cell dysfunction (2,14).

RESEARCH DESIGN AND METHODS

Animal studies. Animal studies were approved by the institutional animal care and use committee at Johns Hopkins University. Mice globally lacking the brain/β-cell EPAC2 isoform EPAC2A (EPAC2A knockout [KO]), prkar1a$^{fl/fl}$, and pancreatic duodenal homeobox-1 CRE mice and their corresponding PCR-based genotyping protocols have been previously described (8,15,16). Interbreeding pancreatic duodenal homeobox-1 CRE and prkar1a$^{fl/fl}$-generated mice lacked pancreas prkar1a (Δprkar1a) (8). Δprkar1a have disinhibited β-cell autonomous PKA catalytic activity and augmented glucose-dependent insulin secretion without changes in EPAC2A levels (8). Glucagon levels in Δprkar1a and controls are similar (8). Compound EPAC2A KO/Δprkar1a mice were generated by interbreeding.

In vivo dynamic tests. Oral and intraperitoneal glucose tolerance tests (oGTT, ipGTT) and insulin tolerance tests (ITT) were performed according to standard protocols (4,17). After 9 A.M. to 3 P.M. fasting, animals were administered 20% D-glucose (2 g/kg orally via gavage or via ip injection) or insulin 0.5 units/kg ip. recombinant human insulin (Novolin, 100 U/mL; Novo Nordisk), respectively. Tail-vein blood was collected at the indicated times in figures for glucose and insulin measurements. To examine in vivo β-cell GSIS after acute E4 (Sigma-Aldrich) administration, mice were treated with 10 nmol/kg E4 or PBS (control) ip 30 min prior to an ipGTT. Plasma glucose was measured using a glucometer (Johnson & Johnson). Serum insulin was measured using mouse magnetic bead panel (Luminex; Millipore).

Immunohistochemistry and pancreas morphometrical analysis. These analyses were performed as previously described (4,17). At least three Bouin-fixed and paraffin-embedded sections per mouse 150 μmol/L apart were immunostained for insulin and analyzed for islet/β-cell mass (4,17). Islet and β-cell mass in wild-type (WT), EPAC2 KO, Δprkar1a, and compound Δprkar1a/EPAC2 KO mice were similar (data not shown), excluding differences in islet mass as a mechanism underlying any differences in GSIS.

Islet isolation. Islet isolation was performed by collagenase digestion, gradient centrifugation, and three rounds of microscope-assisted manual picking of islets (18). Islets were cultured in RPMI 1640 medium (Invitrogen) containing 5 mmol/L D-glucose and supplemented with 1% BSA, 1% HEPES buffer, and 1% penicillin/streptomycin.

Islet perifusion. Islet perifusion was performed on batches of 30 islets with perifusate (1 mL/min) containing 0.2% BSA (4,18). After equilibration for 30 min at 3 mmol/L glucose, perifusate glucose was increased to 10 mmol/L. Insulin was measured in effluent at 30, 35, 40, 42, 45, 50, 55, and 60 min (ELISA; ALPCO Diagnostics). Where indicated, 30 mmol/L KCl was injected at the end of the perifusion protocol to verify that depolarization-induced insulin exocytosis was operational. Area under the curve (AUC) of insulin secretion during perifusion was calculated for the first-phase GSIS (0–10 min) and second-phase GSIS (10–20 min) after raising glucose from 3 to 10 mmol/L. Because of the rapid dynamic changes in insulin secretion with an early nadir at 5 min after glucose stimulus in Δprakar1a and Δprkar1a/EPAC2A KO, first-phase GSIS was considered 0–5 min after raising glucose, with subsequent time points considered as the second phase.

For pharmacologic treatment, islets were exposed to, respectively: E4 10 nmol/L (Sigma-Aldrich), the EPAC-selective activator 8-(4-cholorophenylthio)-2'-*O*-methyladenosine 3′5'-cyclic monophosphate acetoxymethyl ester (ESCA; 10 μmol/L; Biolog Life Science Institute), the PKA-specific cAMP analog activator N6-benzoyladenosine-3′,5′ cyclic monophosphate, acetomethyl ester (6BNZ; 10 μmol/L; Biolog Life Science Institute), the fatty acid receptor free fatty acid 1/GPR40-selective agonist 3-(4-(((3-(phenoxy)phenyl) methyl)amino)phenyl) propionic acid (PMAP; 50 nmol/L; EMD Biosciences), or the PKA-specific inhibitor myristolated PKA inhibitor (PKI; 10 μmol/L; Invitrogen).

Whole-islet calcium dynamics and glucokinase activity. Accounting for heterogenic responses among individual β-cells, we measured the integrated response of glucose-stimulated calcium dynamics in intact cultured islets using a Fura-2 acetoxymethyl ester-based method. Thirty equal-sized islets were incubated in optical microwell dishes (#165306; Nunc) with signal-enhanced ratiometric calcium assay reagents (BD Biosciences) and kept at 3 mmol/L glucose for 1 h (37°C). For treatment with E4 (10 nmol/L) or PMAP (50 nmol/L), islets were exposed to either compound or corresponding vehicle for 1 h before measurements. Measurements were performed in quadruplicate for each islet genotype and/or treatment. Intracellular calcium signals were determined after automated injection of glucose (0.1 M) directly into the culture wells to rapidly increase glucose to 10 mmol/L (Biotek Synergy). Readings (excitation: 340 and 380 nm; emission: 508 nm) were performed at 2-min intervals from the bottom plane. For Fura-2/Ca^{2+}-specific signal, 340/380 nm ratio was calculated. Islet glucokinase (GK) activity was measured in islet extracts as previously described (19).

Islet protein analysis. Immunoblots (IBs) were performed with 40–50 μg protein taken in lysis buffer (Cell Signaling Technology). Protein–protein interaction was assessed by coimmunoprecipitation (Co-IP) followed by IB (Co-IP/IB) of 400–500 μg islet protein lysate. To examine time course of exocytosis-related protein interactions (9), cultured islets were pretreated for 30 min with E4 (10 nmol/L) at 3 mmol/L glucose before acutely increasing the glucose concentration to 10 mmol/L. Thereafter, islets were taken at indicated time points for Co-IP/IB to assess interactions between vesicle-associated soluble N-ethylmaleimide–sensitive factor attachment receptor protein vesicle-associated membrane protein 2 (VAMP2) and target cell membrane–associated SNARE (*t*-SNARE) protein synaptosomal-associated protein 25 (SNAP25) (4). SNAP25–syntaxin 1A interaction was also analyzed to assess SNARE ternary complex assembly. Lysate was incubated at 4°C overnight with antibodies for target cell membrane protein (*t*-SNARE) SNAP25 before adding 250 μl protein A agarose bead slurry (Sigma-Aldrich) for an additional 3 h. Beads were gently spun (pulldown), washed, and taken into 50 μl SDS buffer to detect VAMP2 by IB. For input control, 10% of total protein of corresponding islet lysates served as input controls. Actin served as control for overall protein loading. Densitometric analysis of Co-IP/IB was performed for individual time points.

Short hairpin RNA knockdown studies. Scrambled and murine EPAC1-specific (TR512817; Origene) short hairpin RNA (shRNA)–expressing, purified (Virabind; Invitrogen) lentiviral particles (10^5) were spinoculated (20) twice in polybrene (2 mg/mL; Sigma-Aldrich) with islets. After 3 days in culture, islet insulin secretion assays were performed followed by protein extractions for IB (8).

Quantitative RT-PCR. EPAC1 and EPAC2 isoform mRNA expression was determined by quantitative PCR of islet cDNA using SYBR Green mastermix (Bio-Rad). Primers were: EPAC1 forward, 5′-GGACAAAGTCCCCTACGACA-3′ and reverse, 5′-CTTGGTCCAGTGGTCCTCAT-3′; EPAC2A forward, 5′-TGGAACCAACTGGTATGCTG-3′ and reverse, 5′-CCAATTCCCAGAGTGCAGAT-3′; and EPAC2B forward, 5′-TCTTTGCTACCTGGGACTGG-3′ and reverse, 5′-AGCAGCCAGCCTTTATCTGA-3′. Expression levels were calculated using the $2^{-\Delta\Delta}$ threshold cycle method (21) with 18S rRNA as internal control (forward, 5′-GCAATTATTCCCCATGAACG-3′ and reverse, 5′-GGCCTCACTAAACCATCCAA-3′).

Statistical analysis. Statistical analysis was performed with Prism software (GraphPad). Results are shown as averages and SEM. Where appropriate, Student *t* test or ANOVA and posttest Bonferroni correction were used to calculate differences between groups. $P < 0.05$ was considered significant.

RESULTS

EPAC1 has a small role in GSIS potentiation. Of the two different EPAC genes, EPAC1 mRNA is ubiquitously expressed (22–24). Neurons and β-cells express the EPAC2A splice variant (22–24). Quantitative PCR of mouse islets revealed predominant islet expression of EPAC2A, while 1 and 2B isoform mRNA expression levels were minimal (Fig. 1*A*), confirming previous observations (8,22,25,26). EPAC2A KO islets lack any EPAC2 detectable signal on IB (Fig. 1*B*), further confirming that EPAC2B is not expressed in pancreatic islets (8,22,25). However, EPAC1 protein was detectable on IB of islet protein extracts (Fig. 1*B*). To examine whether EPAC1 participates in GSIS and incretin signaling, we reduced EPAC1 expression by shRNA-mediated knockdown in WT control and EPAC2A KO islets (Fig. 1*B*). EPAC1 knockdown did not significantly influence GSIS (Fig. 1*C*). EPAC1 knockdown in EPAC2A KO islets had no effect on E4-potentiated GSIS as compared with scrambled shRNA-treated islets (Fig. 1*C*). These results suggest that in β-cells, EPAC1 does not regulate GSIS. Islet insulin content was not different between WT or EPAC2A KO islets, and EPAC1 knockdown had no effect on insulin content (Table 1).

Absence of GSIS augmentation by ESCA confirmed lack of EPAC2A function in EPAC2A KO islets (27) (Fig. 1*E*). E4, 6BNZ, and PMAP all potentiated GSIS in WT islets. As expected, E4-stimulated GSIS was blunted in EPAC2A KO

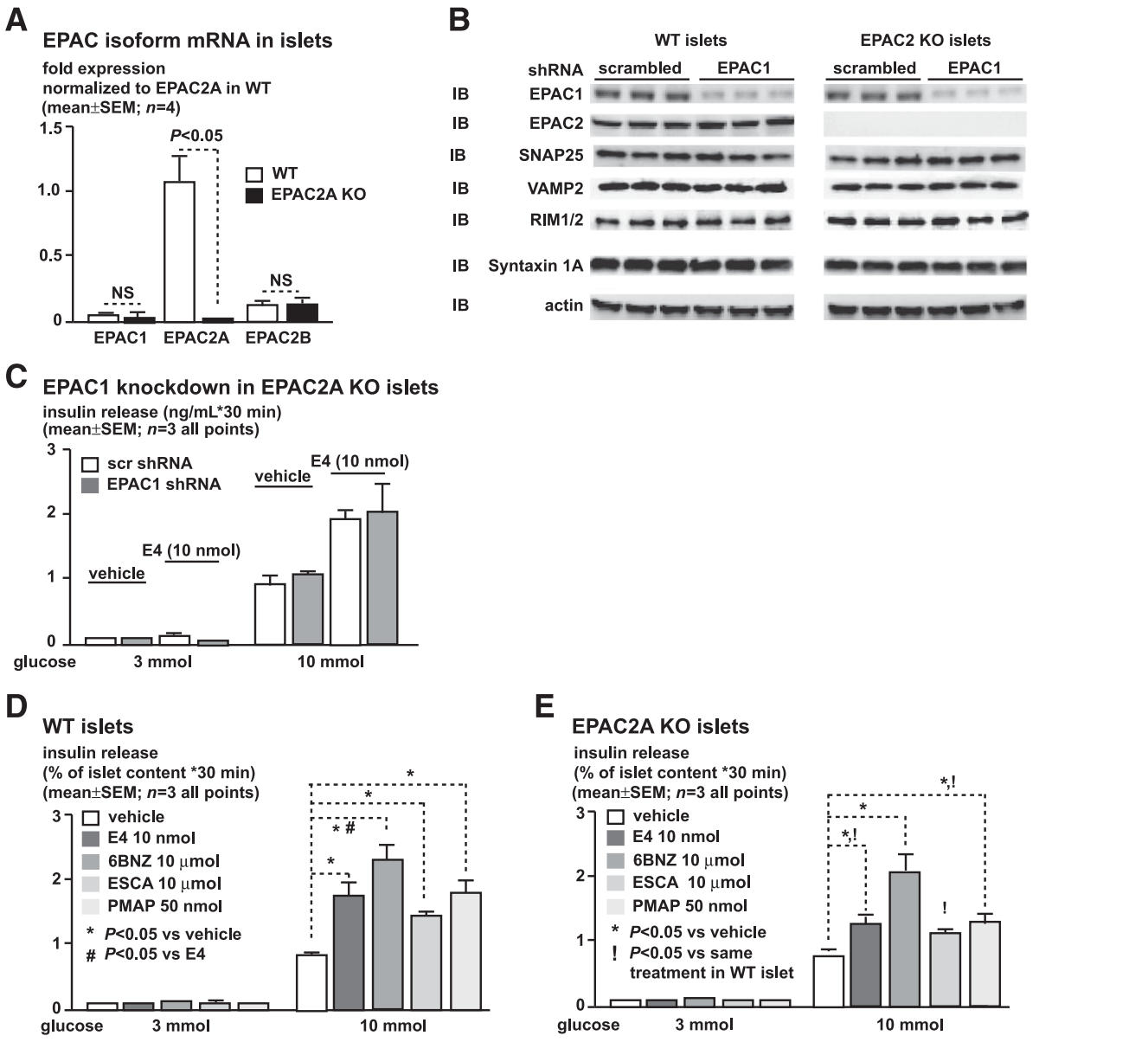

FIG. 1. EPAC1 has a small role in GSIS potentiation. EPAC2A KO islets lack GSIS potentiation in response to pharmacologic secretagogue stimulation. *A*: Quantitative RT-PCR of mouse islets reveals predominant expression of EPAC2A in islets. EPAC1 and EPAC2B isoforms are expressed at low levels and are similar in WT and EPAC2A deficient islets. *B*: shRNA-mediated EPAC1 knockdown in WT and EPAC2A KO islets. IB of islet protein samples shows EPAC1 immunoreactivity in both WT (*left*) and EPAC2A KO (*right*) islets. EPAC2A is present in WT controls and lacking in EPAC2A KO islets. Specific shRNA knockdown specifically reduces EPAC1 immunoreactivity, while no changes were detected with scrambled shRNA. Signals on IB were detected at the expected position corresponding to the molecular weight (Supplementary Table 2). Representative IB is shown with triplicate samples from three different mice for each group. *C*: Insulin-secretion rates during static incubation of EPAC2A KO islets. shRNA-mediated EPAC1 knockdown in EPAC2A KO islets does not impair E4-potentiated GSIS. *Left*: E4 has no effect on insulin secretion at low (3 mmol/L) glucose levels. *Right*: At 10 mmol/L glucose, both scrambled and EPAC1 shRNA-treated islets show similar insulin secretion rates and similarly augment GSIS under E4 (10 nmol/L) exposure. *D*: WT islets secrete insulin in a glucose-dependent manner. Stimulation with incretin hormone analog E4, PKA-selective activator 6BZN, EPAC2-selective activator ESCA, as well as GPR40-selective activator PMAP augment GSIS at 10 but not 3 mmol/L glucose. *E*: EPAC2A KO islets secrete insulin in a glucose-dependent manner. Stimulation with incretin hormone analog E4, PKA-selective activator 6BZN, as well as GPR40-selective activator PMAP augment GSIS. E4 and PMAP augment GSIS to a lesser degree in EPAC2A KO islets (*C*) as compared with WT islets (*D*). EPAC2-selective activator ESCA fails to augment GSIS in EPAC2A KO islets. Vehicle controls: for E4, PBS; for ESCA and PMAP, DMSO. Results are shown as mean ± SEM of triplicate studies. *$P < 0.05$ vs. vehicle, #$P < 0.05$ vs. E4; !$P < 0.05$ for respective treatment EPAC2A KO vs. WT islet (*C* vs. *D*) as determined by two-way ANOVA and Bonferroni posttest analysis. scr, scrambled.

islets (Fig. 1*E*). Interestingly, EPAC2A deficiency impaired GSIS response to PMAP (Fig. 1*E*), indicating an interplay between GPR40 signaling and EPAC2A (see below). EPAC2A KO and WT islets exhibited similar E4-stimulated cAMP generation (Supplementary Fig. 1*A*), while PMAP did not stimulate cAMP (Supplementary Fig. 1*B*). Islet GK activity was similar in WT and EPAC2A KO islets (Supplementary Fig. 1*C*).

EPAC2A deficiency does not influence β-cell mass and results in muted E4-induced GSIS potentiation. Pancreas morphometric analyses of 6-week-old WT and EPAC2A KO littermates showed no differences in pancreas weight, β-cell mass, β-cell size, or insulin content (Table 1).

Both oGTT and ipGTT were similar in WT and EPAC2A KO littermates kept on regular rodent diet, consistent with previous observations (5) (Fig. 2*A* and *B*). Under these

TABLE 1
Morphometric analysis, islet insulin content, and EPAC isoform expression of WT and EPAC2A KO littermates

	WT	EPAC2A KO	*P* value
Morphometry			
Pancreas weight (mg)	256 ± 11.8	239 ± 6.9	NS
β-cell mass (mg)	1.1 ± 0.3	1.1 ± 0.2	NS
β-cell size (μm^2)	129 ± 3	129 ± 3	NS
Islet insulin content (ng/μg protein)			
Scrambled RNA	165 ± 17	169 ± 14	NS
EPAC1 shRNA	173 ± 17	168 ± 11	NS

Data are mean ± SEM. $n = 3$. Pancreas weight, β-cell mass, and size are similar in 6-week-old male WT and EPAC2A KO mice in the C57Bl/6 background. Islet insulin content (50 islets/assay) normalized to total islet protein is similar in WT and EPAC2A KO mice with or without EPAC1 shRNA-mediated knockdown.

basal conditions, insulin secretion during ipGTT was similar in EPAC2A KO and WT littermates (Fig. 2*C*). A slight increase in insulin sensitivity was noted in EPAC2A-deficient mice as compared with controls (Fig. 2*D*). Isolated islets from EPAC2A KO and WT littermates exhibited similar insulin secretion patterns during perifusion studies (Fig. 2*E* and Supplementary Table 1) as well as similar glucose-stimulated changes in iCa^{2+} (Fig. 2*F* and *G*).

In contrast to the above baseline findings, when stimulated with ip E4 administration during ipGTT, EPAC2A KO mice exhibited a slower decline of serum glucose levels (Fig. 3*A*). The impaired GTT in EPAC2A KO mice was reflected by a diminished response to E4-mediated GSIS potentiation in EPAC2A KO versus control mice (Fig. 3*B*).

Perifusion studies of control and EPAC2A KO islets mirrored the in vivo observations on insulin secretion. During pharmacologic stimulation with E4, EPAC2A KO islets exhibited significantly reduced GSIS potentiation, which was most pronounced during the first phase of the secretory response (Fig. 3*C* and Supplementary Table 1). Integrated islet calcium dynamics of E4-stimulated EPAC2A KO and WT islets were similar at low glucose levels (Fig. 3*D*). When stimulated with glucose plus E4, WT islets exhibited a robust response of iCa^{2+} primarily in the initial phases after glucose stimulation (Fig. 3*E*). In contrast, EPAC2A KO islets failed to exhibit the dramatic response in iCa^{2+} observed in control islets (Fig. 3*E*). These results suggest that while EPAC2A function appears dispensable during basal GSIS, EPAC2A is required when β-cell insulin secretion is potentiated by pharmacologic (i.e., supraphysiologic, in contrast to physiologic) GLP-1R activation.

Co-IP studies of proteins involved in insulin vesicle exocytosis (9) showed increased interaction of the cell membrane–bound *t*-SNARE protein SNAP25 with syntaxin 1A and with the vesicle-bound (vesicle-associated soluble N-ethylmaleimide–sensitive factor attachment receptor) protein VAMP2 in E4-pretreated WT islets within minutes after exposure to elevated glucose levels (10 mmol/L). In contrast, EPAC2A KO islets showed during identical studies a weaker and delayed SNAP25–VAMP2 and SNAP25–syntaxin 1A interactions. (Supplementary Fig. 2). The time course of this protein interaction correlates with the observations made in intracellular calcium dynamics as well as insulin secretion during perifusion studies. These findings are consistent with previous observations that insulin exocytosis requires an increase in intracellular calcium (9), which, as found in this study, is delayed in glucose- and E4-stimulated EPAC2A KO islets.

EPAC2A is required for increased β-cell functional response to diet-related insulin resistance. Based on these observations, we reasoned that EPAC2A function may be required for enhancing β-cell secretory response not only when pharmacologically stimulated with GLP-1R agonist but also under conditions when metabolic demands on insulin secretion are increased. We exposed mice to 4 weeks of high-fat diet (HFD) in order to achieve diet-induced insulin resistance. During HFD feeding, EPAC2A KO and WT mice did not exhibit any differences in weight gain (data not shown), indicating that EPAC2A deficiency has no effect on weight regulation during this short-term caloric surfeit. Interestingly, HFD-fed EPAC2A KO, as compared with controls, exhibited impaired glucose tolerance and diminished insulin secretion during ipGTT (Fig. 4*A* and *B*). As with the normal diet–fed mice, ITT revealed slightly increased insulin sensitivity in EPAC2A KO mice as compared with controls (Fig. 4*C*). Despite increased insulin sensitivity, EPAC2A KO mice exhibited impaired glucose tolerance as compared with WT, indicating a limitation in their insulin secretion (Fig. 4*A* and *B*). Perifusion studies confirmed a reduction in GSIS in HFD-fed EPAC2A KO islets relative to controls (Fig. 4*D* and Supplementary Table 1). EPAC2A deficiency mainly resulted in reduction of the first phase of GSIS, while the second phase of GSIS was remarkably similar in HFD-fed EPAC2A KO and WT mouse islets (Fig. 4*D*). The observations made during perifusion studies were mirrored in integrated islet calcium dynamics. HFD-fed EPAC2A KO mouse islets exhibited, as compared with controls, diminished glucose-induced iCa^{2+} increase primarily during the initial rise after glucose stimulation (Fig. 4*E* and *F*).

EPAC2A is required for enhancing insulin secretion in a model of β-cell autonomous GSIS potentiation. Besides inducing insulin resistance, HFD may cause additional confounding effects on β-cell function (28,29). We therefore sought to examine EPAC2A function in a genetic model of β-cell autonomous GSIS potentiation. Mice with disinihibited PKA in their islets (Δprkar1a mice) exhibit dramatically (5–10-fold) enhanced GSIS without hypoglycemia or change in islet mass (4). We interbred Δprkar1a and EPAC2A KO mice to generate compound Δprkar1a/EPAC2A KO mice. As expected, islet prkar1a ablation resulted in significantly improved glucose tolerance (Fig. 5*A*). GSIS was significantly reduced in Δprkar1a/EPAC2A KO as compared with Δprkar1a mice (Fig. 5*B*). Albeit, the very high insulin secretory response resulting from prkar1a ablation was sufficient to keep glucose tolerance similar in both Δprkar1a and Δprkar1a/EPAC2A KO mice (Fig. 5*A*

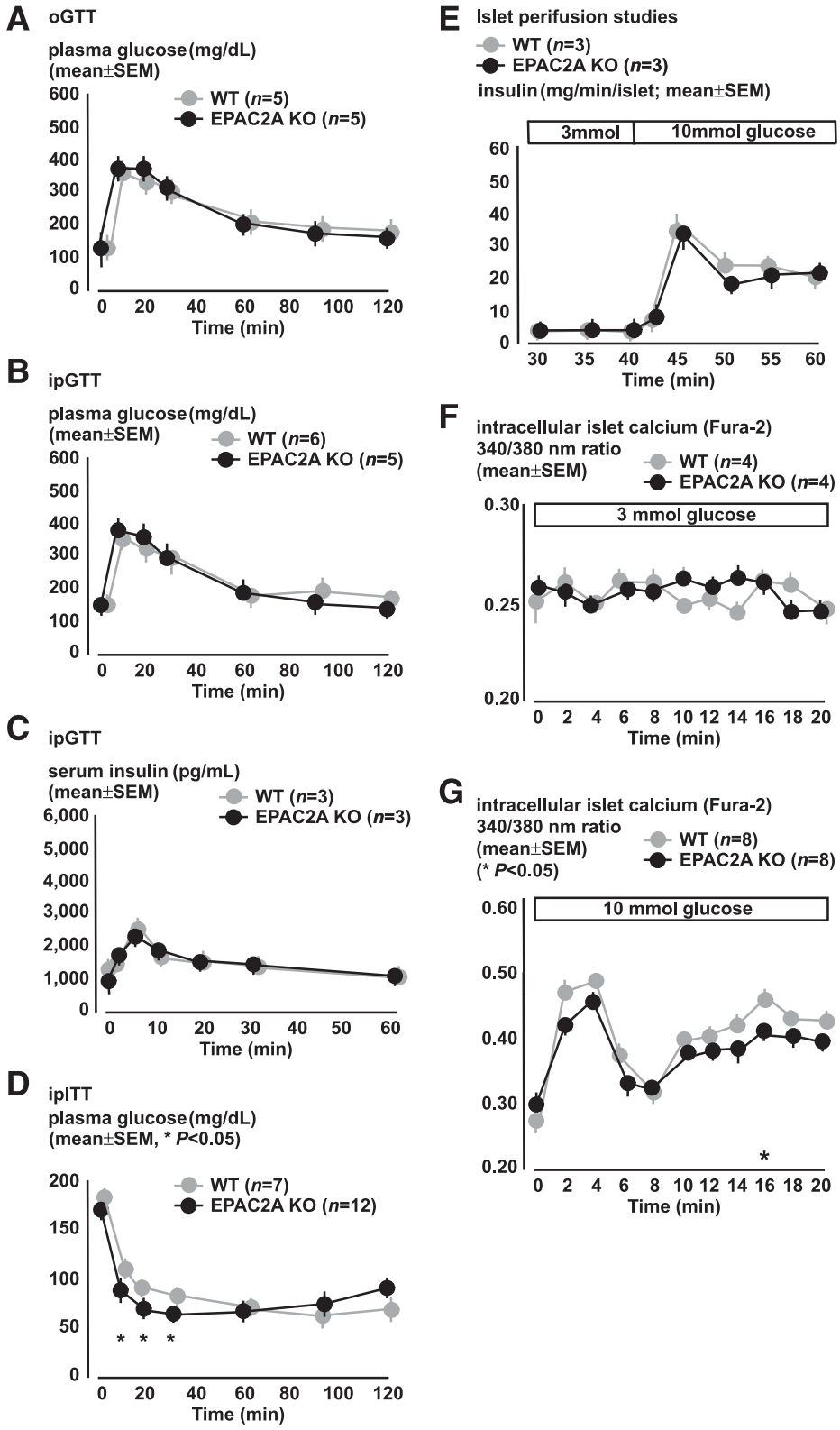

FIG. 2. EPAC2A ablation does not influence GSIS. *A–D*: In vivo studies. *E* and *F*: In vitro studies. EPAC2A KO mice and WT controls have similar glucose excursions during oGTT (*A*) and ipGTT (*B*). *C*: Serum insulin levels during ipGTT are not different in WT and EPAC2A KO mice. *D*: ipITT shows slightly increased insulin sensitivity in EPAC2A KO mice as compared with controls. *E*: WT and EPAC2A KO islets show similar insulin secretion rates during perifusion studies. *F* and *G*: Islet intracellular calcium dynamic changes detected with the Fura-2 method in EPAC2A KO and WT islets are similar. *F*: Islets maintained in 3 mmol/L glucose show no differences in intracellular calcium levels. *G*: Increasing glucose levels from 5 to 10 mmol/L at time 0 min elicits an increase in intracellular calcium signal, which is similar in WT and EPAC2A KO islets. WT is represented in gray circles; EPAC2A KO is represented in black circles. Results are shown as mean ± SEM of studies performed at least in triplicate. *$P < 0.05$.

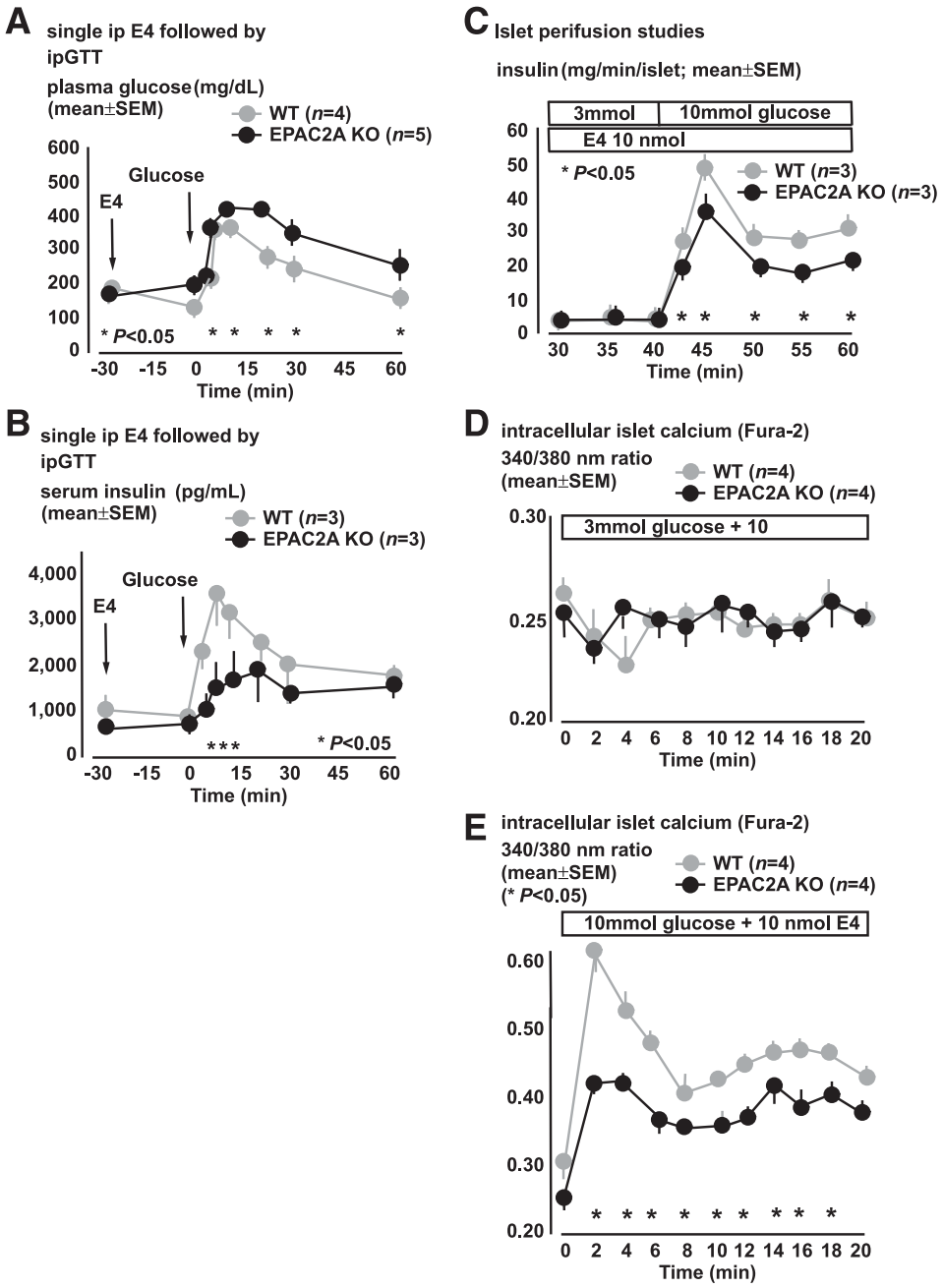

FIG. 3. EPAC2A ablation impairs dynamic insulin response to E4-mediated GSIS potentiation. *A* and *B*: In vivo studies. *C–E*: In vitro studies. *A*: Acute E4 administration prior to ipGTT reveals relatively improved glucose tolerance in WT as compared with EPAC2A KO mice. *B*: Acute E4 administration prior to ipGTT elicits augmented GSIS in WT mice, while E4-stimulated GSIS augmentation is lacking in EPAC2A KO counterparts. *C*: Perifusion studies show E4-stimulated GSIS augmentation in WT islets, which is muted in EPAC2A KO islets. *D* and *E*: Islet intracellular calcium dynamic changes detected with the Fura-2 method in EPAC2A KO and WT islets. *D*: Islets maintained in 3 mmol/L glucose show no differences in intracellular calcium levels. *E*: Increasing glucose levels from 5 to 10 mmol/L at time 0 min elicits an increase in intracellular calcium signal, which is reduced in EPAC2A KO islets as compared with WT control islets. WT is represented in gray circles; EPAC2A KO is represented in black circles. Results are shown as mean ± SEM of studies performed at least in triplicate. *$P < 0.05$.

and *B*). Insulin sensitivity as assessed by intraperitoneal ITT (ipITT) did not differ between Δprkar1a and Δprkar1a/EPAC2A KO mice (Fig. 5*C*).

Perifusion studies showed dramatically augmented GSIS in Δprkar1a islets (Fig. 5*D* and Supplementary Table 1), reflecting in vivo observations. Δprkar1a/EPAC2A KO islets also showed increased GSIS as compared with EPAC2A KO islets (Fig. 2*E*). However, as compared with Δprkar1a islets, compound Δprkar1a/EPAC2A KO islets exhibited a blunted first-phase GSIS. This finding suggests that EPAC2A function, while not critical, is required for the cAMP–PKA signaling branch to be fully effective in GSIS augmentation.

Δprkar1a islets exhibited increased islet iCa^{2+} in response to a glucose stimulus, which paralleled the dynamics in insulin secretion found during perifusion. Compared with controls, Δprkar1a/EPAC2A KO islets exhibited muted iCa^{2+} excursions, primarily in the initial phase after glucose stimulation (Fig. 5*E* and *F*). When additionally exposed to 4 weeks of HFD, Δprkar1a mice responded with further enhanced

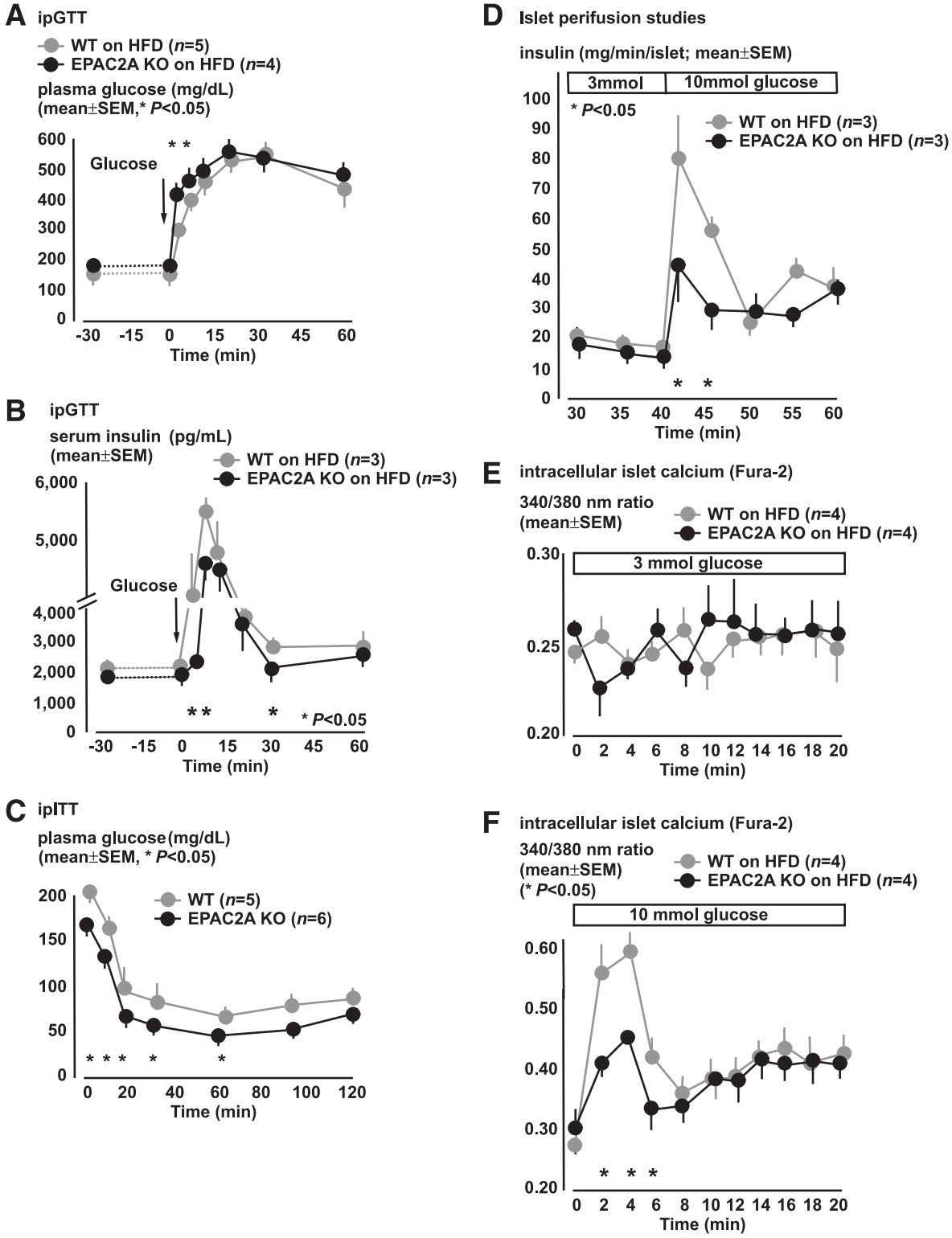

FIG. 4. EPAC2A ablation impairs dynamic insulin response in diet-induced obesity and insulin resistance model. *A–C*: In vivo studies. *D–F*: In vitro studies. *A*: HFD-fed WT mice show impaired ip glucose tolerance, which is more pronounced in HFD-fed EPAC2A KO mice. *B*: HFD-fed WT mice show augmented serum insulin excursions in response to ip glucose. In comparison, EPAC2A KO mice show a delayed and impaired insulin response to ip glucose. *C*: HFD-fed EPAC2A KO mice, as compared with WT controls, show slightly increased insulin sensitivity, which does not compensate their impaired glucose tolerance (*A*). *D*: Perifusion studies of islets from HFD-fed mice show GSIS augmentation in WT islets, which is blunted in EPAC2A KO islets mainly in the early phases (40–45 min) after glucose stimulus to the islets. *E* and *F*: Islet intracellular calcium dynamic changes detected with the Fura-2 method in EPAC2A KO and WT islets of HFD-fed mice. *E*: Islets maintained in 3 mmol/L glucose show no differences in intracellular calcium levels. *F*: Increasing glucose levels from 3 to 10 mmol/L at time 0 min elicits an increase in intracellular calcium signal. EPAC2A KO islets show a blunted early (0–10 min) rise in glucose-stimulated intracellular calcium, which, at later time points (10–20 min), is similar in WT and EPAC2A KO islets. WT is represented in gray circles; EPAC2A KO is represented in black circles. Results are shown as mean ± SEM of studies performed at least in triplicate. *$P < 0.05$.

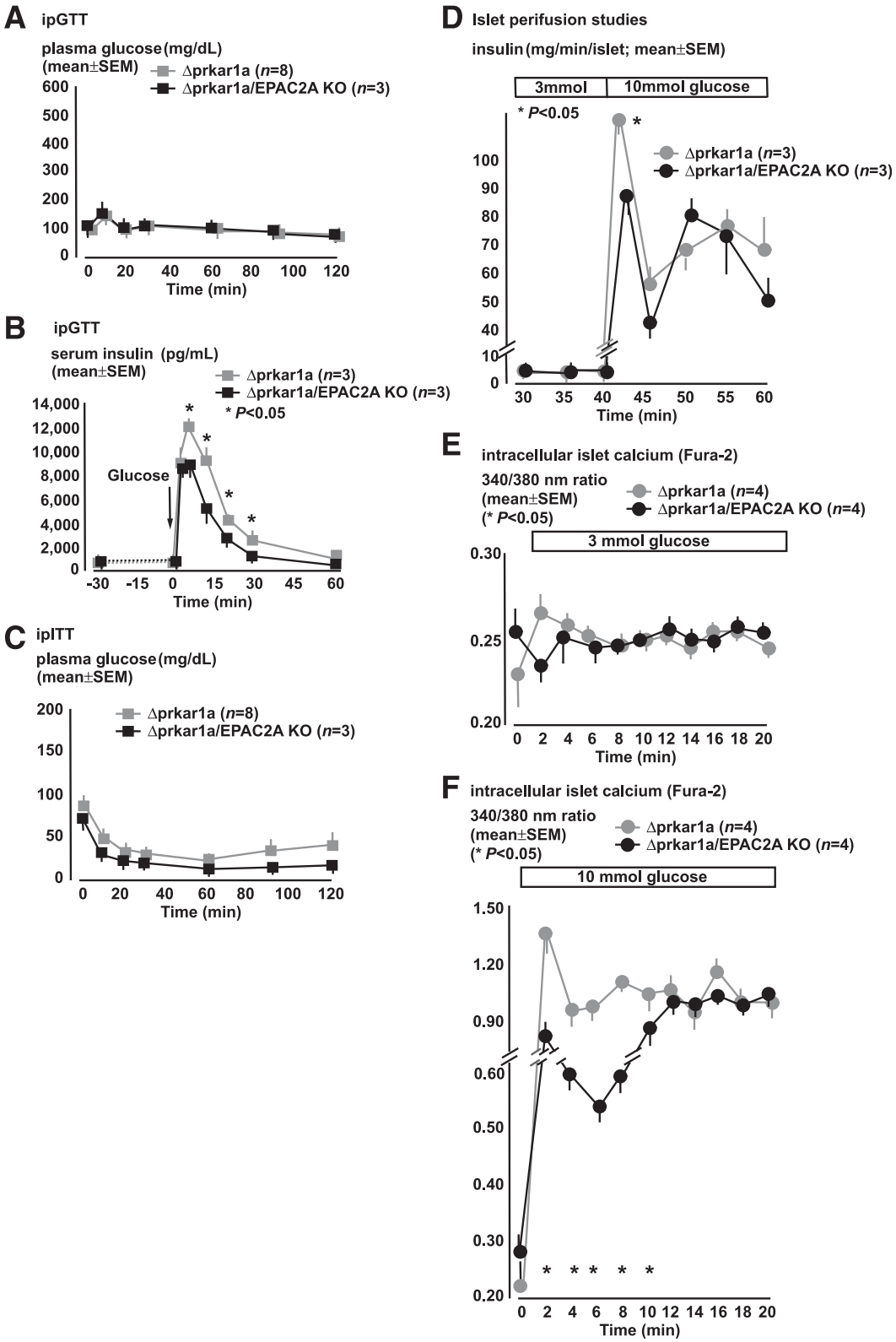

FIG. 5. EPAC2A ablation impairs dynamic insulin response in model of β-cell autonomous GSIS augmentation (Δprkar1a mice). *A–C*: In vivo studies. *D–F*: In vitro studies. *A*: During ipGTT, Δprkar1a and Δprkar1a/EPAC2A KO mice exhibit similar glucose excursions. *B*: During ipGTT, Δprkar1a show, as compared with WT mice (Fig. 3), dramatically increased GSIS. Δprkar1a/EPAC2A KO mice exhibit reduced serum insulin levels as compared with Δprkar1a mice. *C*: During ipITT, Δprkar1a/EPAC2A KO, as compared with Δprkar1a mice, show slightly increased insulin sensitivity, which does not reach statistical significance. *D*: Perifusion studies of islets from Δprkar1a and Δprkar1a/EPAC2A KO mice. Δprkar1a islets exhibit a dramatically augmented GSIS. In contrast, Δprkar1a/EPAC2A KO islets exhibit a relatively blunted first-phase GSIS, while second-phase GSIS is similar in both groups. *E* and *F*: Islet Intracellular calcium dynamic changes detected with the Fura-2 method in Δprkar1a and Δprkar1a/EPAC2A KO islets. *E*: Islets maintained in 3 mmol/L glucose show no differences in intracellular calcium levels. *F*: Increasing glucose

in vivo GSIS, whereas Δprkar1a/EPAC2A KO counterparts exhibited blunted insulin secretion with a near complete absence of first-phase insulin secretion (Supplementary Fig. 3).

Taken together, these findings suggest that EPAC2A is required for augmenting GSIS either in response to diet-related insulin resistance, to pharmacologic β-cell secretagogue stimulation, or in conditions of β-cell autonomous GSIS potentiation.

PKA activity is essential for overall GSIS, and EPAC2A predominantly augments first phase of E4-stimulated GSIS. To further dissect the interplay between PKA- and EPAC2A-dependent signaling in GSIS, we introduced pharmacologic manipulation of cAMP–PKA and cAMP–EPAC2 pathways during perifusion studies. Stimulation with the PKA-selective cAMP agonist 6BZN increased GSIS in both WT and EPAC2A KO islets. However, the immediate early rise in GSIS after the glucose stimulus was significantly blunted in EPAC2A KO islets (Supplementary Fig. 4*A*). EPAC2A-selective activation with ESCA was met with a blunted GSIS in EPAC2A KO islets (Supplementary Fig. 4*B*). This was pronounced during the first phase and persisted during the second phase of insulin secretion (Supplementary Fig. 4*B* and Supplementary Table 1).

In contrast, PKI treatment abolished all GSIS except for a small residual insulin release early after glucose exposure (Supplementary Fig. 4*C*). Stimulation with E4 or with ESCA did not reverse the inhibitory effects of PKI (Supplementary Fig. 4*D* and *E*), confirming previous observations that PKA activity is required for EPAC2A-mediated GSIS potentiation (6). PMAP stimulation had a clear but modest effect on GSIS despite PKI inhibition of PKA in WT islets. In contrast, PMAP potentiation of GSIS was absent in PKI-treated EPAC2A KO islets, suggesting that PMAP and EPAC2A may in part interact in a PKA-independent manner (Supplementary Fig. 4*F*) (see also below). Depolarizing PKI-treated islets with KCl-stimulated insulin release, indicating that despite PKI inhibition, islets maintained exocytosis capability (Supplementary Fig. 4*C* and *D*). The mechanism underlying the small, albeit distinct, early burst of insulin output seen during PKI treatment remains unclear and is likely directly stimulated by glucose. Taken together, these studies indicate that in β-cells, while the cAMP–PKA branch is sufficient to augment GSIS, it requires EPAC2A for a maximal response.

EPAC2A absence diminishes GPR40-mediated GSIS. GPR40 is expressed at high density on β-cells. Pharmacologic activation of GPR40, similarly to incretin hormone receptor activation, potentiates GSIS, with no insulin secretion when glucose is below physiologic fasting levels (12,13,30,31). Initial pharmacologic trials in humans with GPR40-selective activators indicate their effectiveness in ameliorating insulin secretion and glycemia in T2DM (30).

We examined whether EPAC2A function may also be relevant in GPR40-mediated GSIS augmentation, which is distinct from GLP-1R activation and cAMP signaling (12,13). During perifusion, WT islets exposed to the GPR40-selective agonist PMAP potentiated GSIS, confirming previous observations GPR40 action in the islet (12,13). In contrast, GPR40 activation in EPAC2A KO islets resulted in significantly reduced first-phase GSIS (Fig. 6*A*). PMAP-stimulated islet iCa^{2+} in a glucose-dependent manner as previously described (12,13). Interestingly, EPAC2A KO islets, as compared with controls, exhibited a reduced PMAP-induced rise in iCa^{2+} levels (Fig. 6*B* and *C*), Together with the observation that PMAP does not stimulate cAMP synthesis in islets (Supplementary Fig. 1), these observations suggest that EPAC2A function may only in part be related to its incretin-stimulated cAMP-dependent activation and that EPAC2A has a wider role in potentiating GSIS in response to other stimuli.

To examine a potential interplay between GPR40- and PKA-mediated GSIS augmentation, we inhibited PKA activity with the selective inhibitor PKI in islets exposed to PMAP (Supplementary Fig. 4*E*). PKA inhibition did not influence PMAP-potentiated GSIS. PKI-mediated inhibition in EPAC2A KO islets completely abolished PMAP-induced GSIS stimulation (Supplementary Fig. 4*F*), suggesting a dependency of GPR40-mediated GSIS stimulation on overall intact cAMP-dependent signaling. Taken together, these findings suggest that GPR40-mediated GSIS potentiation requires EPAC2A function to be fully effective.

DISCUSSION

The present in vivo studies of genetically defined mouse models combined with in vitro examination of their islets suggest an important role for EPAC2A function during increased demand on insulin secretion by the β-cell. Our studies expand the conceptual understanding of EPAC2A function beyond its role in mediating cAMP-dependent effects of pharmacological GLP-1R activators (i.e., E4). While EPAC2A appears to have little significance during basal conditions (Fig. 3*A*–*E*), EPAC2A function becomes relevant in circumstances of increased demand on β-cell GSIS.

To our knowledge, this is the first report of a direct in vivo examination of pharmacologic incretin analog E4 action in EPAC2A KO mice. In EPAC2A-deficient mice as compared with controls, E4 effects on GSIS potentiation are markedly reduced (Fig. 3*A* and *B*). Perifusion (Fig. 3*D*) and islet iCa^{2+} studies (Fig. 3*E* and *F*) reveal that during pharmacologic E4 stimulation, EPAC2A is required predominantly for augmenting the initial burst of iCa^{2+}, which is associated with a corresponding GSIS potentiation. Furthermore, EPAC2A deficiency is associated with delayed interaction of insulin vesicle exocytosis-associated proteins SNAP25 and VAMP2 (Supplementary Fig. 2). These findings are consistent with the observation that a rise in iCa^{2+} is required for exocytosis to occur (9). EPAC2A deficiency delays the increase in iCa^{2+} (Fig. 3*F*) after glucose stimulation, which compromises insulin exocytosis (i.e., secretion) (Fig. 3*D*).

The unexpected observation of slightly increased insulin sensitivity in EPAC2A mice may confound in vivo observations on insulin secretion. This prompted us to include in vitro studies in isolated islets, thereby ensuring a direct assessment of EPAC2A function in β-cells. Of note, EPAC2A may exert a role in non–β-pancreatic islet cells (32), which may additionally influence β-cell function. In

levels from 3 to 10 mmol/L at time 0 min elicits a dramatic increase in intracellular calcium signal in Δprkar1a islets. Δprkar1a/EPAC2A KO islets show a blunted early (0–10 min) rise in glucose-stimulated intracellular calcium, which, at later time points (10–20 min), is similar in both groups. Δprkar1a is represented in gray circles; Δprkar1a/EPAC2A KO is represented in black circles. Results are shown as mean ± SEM of studies performed at least in triplicate. *$P < 0.05$.

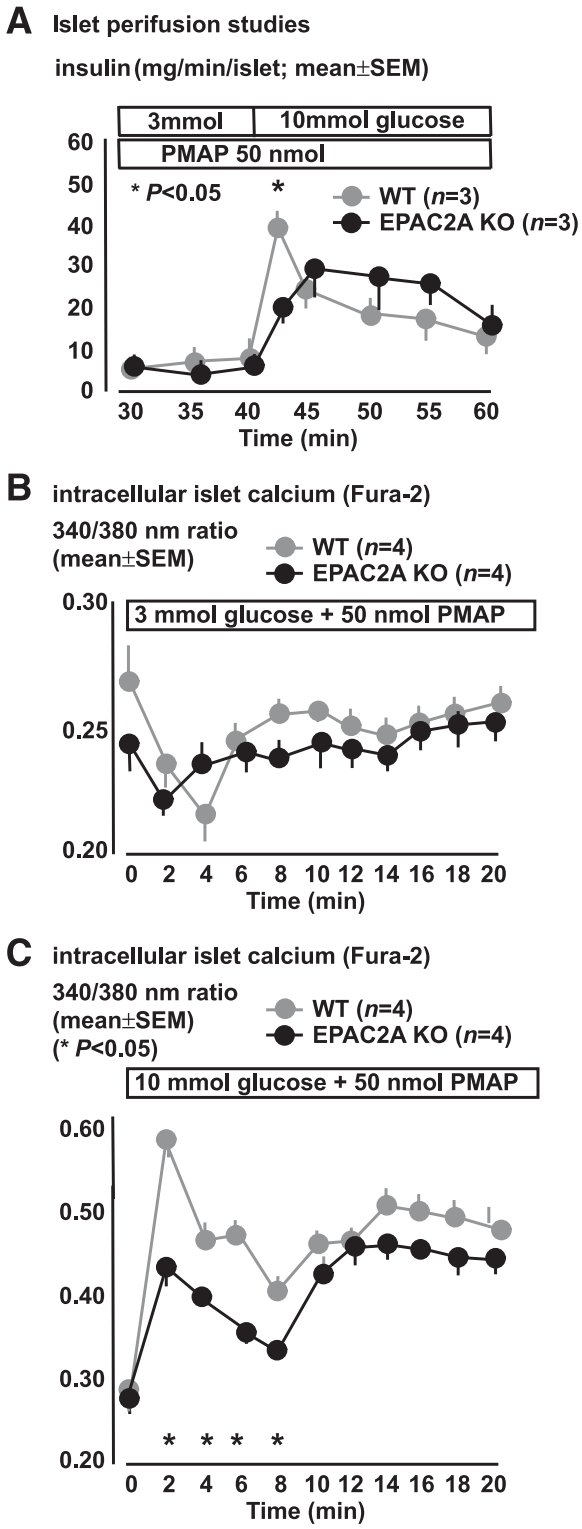

FIG. 6. EPAC2A ablation impairs GSIS augmentation in response to free fatty acid 1/GRP40 activation. *A*: Perifusion studies of PMAP-treated islets GSIS augmentation in WT islets, which is blunted in EPAC2A KO islets mainly in the acute phase (40–42 min) after glucose stimulus to the islets, while later time points show similar insulin secretion in WT and EPAC2A KO islets. *B* and *C*: Islet intracellular calcium dynamic changes detected with the Fura-2 method in PMAP-treated WT and EPAC2A KO islets. *B*: Islets maintained in 3 mmol/L glucose show no differences in intracellular calcium levels. *C*: Increasing glucose levels from 3 to 10 mmol/L at time 0 min elicits an increase in intracellular calcium signal in WT islets. EPAC2A KO islets show a blunted early (0–10 min) rise in glucose-stimulated intracellular calcium, which, at later time points (10–20 min), is similar in both groups. WT is represented in gray circles; EPAC2A KO is represented in black circles. Results are shown as mean ± SEM of studies performed at least in triplicate. *$P < 0.05$.

this context, future studies with conditional cell–specific EPAC2A ablation will be necessary to specifically separate in vivo β-cell from non–β-cell islet effects or from peripheral tissue effects of EPAC2A.

The role for EPAC2A in potentiating GSIS was also observed in the diet-induced obesity and insulin resistance model. When kept on a normal laboratory mouse diet, EPAC2A-deficient mice and their islets, as compared with normal littermates, showed no differences in glucose homeostasis, insulin secretion, and islet iCa^{2+} dynamics (Fig. 2). Conversely, HFD-fed insulin-resistant mice exhibited augmented GSIS during GTT, reflecting the β-cell response to increased metabolic demand. Under HFD conditions, EPAC2A KO mice exhibited defective GSIS and glucose tolerance (Fig. 4*A*–*C*), indicating that EPAC2A function becomes relevant under increased demand on β-cell secretion. These dynamic changes in insulin secretion were reflected in EPAC2A KO islets mainly by a reduction of the initial increase in intracellular calcium levels after glucose stimulation. Thus, EPAC2A absence aggravates β-cell dysfunction in the face of diet-induced insulin resistance.

How β-cells sense increased insulin resistance and respond to the increased metabolic demand on insulin secretion remains unclear (1). To this end, the present studies suggest that EPAC2A occupies an important role in the molecular mechanisms of β-cell adaptation to increased secretory demand. Conversely, we speculate that in T2DM, EPAC2A function may be compromised and contribute toward failure of β-cells to compensate for increased demand (33).

When examining the interplay of the cAMP–PKA and cAMP–EPAC2A branches of GLP-1R signaling, β-cell autonomous disinhibition of the cAMP–PKA branch (Δprkar1a mice) is sufficient to potentiate GSIS (Fig. 5*B*). However, EPAC2A function is required for PKA activity to reach optimal stimulation of iCa^{2+} dynamics and GSIS (Fig. 5*B*, *D*, and *E*). When β-cells are further stimulated to augment GSIS by a combination of islet PKA disinhibition plus HFD-induced insulin resistance, EPAC2A absence significantly blunts first-phase insulin secretion (Δprkar1a/EPAC2A KO mice; Supplementary Fig. 3*C*). Conversely, inhibition of PKA catalytic activity with the PKA-selective inhibitor PKI abolishes GSIS elicited by E4 or by the EPAC2A-selective activator (ESCA; Supplementary Fig. 4*D* and *E*). Based on these studies, we conclude that PKA activity is essential for GSIS. Further, while EPAC2A cannot function independently of PKA, EPAC2A is required and permissive for optimal GSIS potentiation when PKA-dependent signaling is activated.

The signal transduction pathways engaged by the G protein–coupled GPR40 receptor and mediated by Gaq/11, while resulting in increased in iCa^{2+} (31), have thus far not been considered to interplay with EPAC2A. However, the present studies suggest that GPR40 agonist-mediated GSIS potentiation requires functional EPAC2A (Fig. 6*A* and Supplementary Fig. 4*F*). Islet EPAC2A function is required, at least in part, to amplify the rise in iCa^{2+} levels stimulated by GP40 action (Fig. 6*C*). Both GPR40 and EPAC2A activate different phospholipase C isoforms (31,34,35), which in turn hydrolyze phosphoinositol 4,5, bisphosphate to diacylglycerol and inositol trisphosphate (IP3). IP3 engages the endoplasmatic reticulum IP3 receptor, leading to the opening of Ca^{2+} release channels. The Ca^{2+} release channels allow endoplasmatic reticulum–stored Ca^{2+} to exit into the cytoplasm, thereby potentiating an increase in cytoplasmic iCa^{2+} levels (35). It is thus conceivable that GPR40- and EPAC2A-dependent signaling converge at Ca^{2+} release channels in a complementary manner. Our observations suggest that EPAC2A potentiates GPR40-dependent Ca^{2+} mobilization early after glucose-stimulated β-cells (Fig. 6*C*). GPR40 stimulation does not increase cAMP levels in β-cells (Supplementary Fig. 1) (12,13), making it unlikely that GPR40 activation directly stimulates EPAC2A.

The present findings do not exclude EPAC2A-independent mechanisms in dynamic changes in β-cell cytoplasmic iCa^{2+}. Our findings also do not exclude additional functions of EPAC2A related to insulin secretion such as regulating the pool of vesicles destined for exocytosis (36,37). Detailed future studies will be necessary to elucidate role of EPAC2A on subcellular events within the β-cell. Nevertheless, our studies suggest that EPAC2A plays an important role in augmenting iCa^{2+} levels when β-cells face an increased demand to secrete insulin. This model is consistent with and extends the models of EPAC2A-mediated closure of the K-ATP channel, resulting in voltage-dependent influx of extracellular Ca^{2+} into β-cells (38–40) as well as EPAC2A-mediated calcium-induced calcium release from intracellular compartments (7,41,42). Our observations are also compatible with findings that EPAC2A is activated at cAMP concentrations, which are several-fold higher than those that activate PKA (10,11). Thus, during physiologic incretin stimulation of β-cells, the cAMP–PKA signaling branch may be predominantly activated without significantly engaging the cAMP–EPAC2A branch. In contrast, during pharmacologic β-cell GLP-1 receptor activation (i.e., E4 treatment), larger concentrations of cAMP may be generated, which activate EPAC2A in addition to stimulating PKA.

In a broader context, our findings may guide development and tailored administration of pharmacologic therapy for human T2DM. EPAC2A-specific stimulation may improve dynamic GSIS in insulin-resistant and prediabetic patients (36). Furthermore, combination of GPR40 agonists with EPAC2A-selective or GLP-1R activators tailored to specific patients' needs may show synergistic effects on reversing β-cell dysfunction (2).

ACKNOWLEDGMENTS

This work was supported by grants from the National Institutes of Health (DK-090245, DK-090816, DK-084949, and DK-079637).

No potential conflicts of interest relevant to this article were reported.

W.-J.S., P.M., Y.L., and S.E.L. researched data. M.A.H. designed study, researched data, and wrote the manuscript. M.A.H. is the guarantor of this work and, as such, had full access to all the data in the study and takes responsibility for the integrity of the data and the accuracy of the data analysis.

The authors thank A. Wolfe and F. Wondisford, Johns Hopkins University, for editorial assistance and Constantine Stratakis (National Institute of Child Health and Human Development) and Lawrence Kirschner (Columbus University) for $prkar1a^{fl/fl}$ and Susumu Seino (Kobe University) for EPAC2A KO mice.

REFERENCES

1. Cavaghan MK, Ehrmann DA, Polonsky KS. Interactions between insulin resistance and insulin secretion in the development of glucose intolerance. J Clin Invest 2000;106:329–333
2. DeFronzo RA, Abdul-Ghani MA. Preservation of β-cell function: the key to diabetes prevention. J Clin Endocrinol Metab 2011;96:2354–2366

3. Drucker DJ. The biology of incretin hormones. Cell Metab 2006;3:153–165
4. Song WJ, Seshadri M, Ashraf U, et al. Snapin mediates incretin action and augments glucose-dependent insulin secretion. Cell Metab 2011;13:308–319
5. Zhang CL, Katoh M, Shibasaki T, et al. The cAMP sensor Epac2 is a direct target of antidiabetic sulfonylurea drugs. Science 2009;325:607–610
6. Chepurny OG, Kelley GG, Dzhura I, et al. PKA-dependent potentiation of glucose-stimulated insulin secretion by Epac activator 8-pCPT-2′-O-Me-cAMP-AM in human islets of Langerhans. Am J Physiol Endocrinol Metab 2010;298:E622–E633
7. Kang G, Chepurny OG, Rindler MJ, et al. A cAMP and Ca2+ coincidence detector in support of Ca2+-induced Ca2+ release in mouse pancreatic beta cells. J Physiol 2005;566:173–188
8. Shibasaki T, Takahashi H, Miki T, et al. Essential role of Epac2/Rap1 signaling in regulation of insulin granule dynamics by cAMP. Proc Natl Acad Sci USA 2007;104:19333–19338
9. Südhof TC, Rothman JE. Membrane fusion: grappling with SNARE and SM proteins. Science 2009;323:474–477
10. Døskeland SO, Ogreid D. Binding proteins for cyclic AMP in mammalian tissues. Int J Biochem 1981;13:1–19
11. Ekanger R, Sand TE, Ogreid D, Christoffersen T, Døskeland SO. The separate estimation of cAMP intracellularly bound to the regulatory subunits of protein kinase I and II in glucagon-stimulated rat hepatocytes. J Biol Chem 1985;260:3393–3401
12. Salehi A, Flodgren E, Nilsson NE, et al. Free fatty acid receptor 1 (FFA(1) R/GPR40) and its involvement in fatty-acid-stimulated insulin secretion. Cell Tissue Res 2005;322:207–215
13. Tan CP, Feng Y, Zhou YP, et al. Selective small-molecule agonists of G protein-coupled receptor 40 promote glucose-dependent insulin secretion and reduce blood glucose in mice. Diabetes 2008;57:2211–2219
14. Seino S, Takahashi H, Takahashi T, Shibasaki T. Treating diabetes today: a matter of selectivity of sulphonylureas. Diabetes Obes Metab 2012;14 (Suppl. 1):9–13
15. Lammert E, Cleaver O, Melton D. Induction of pancreatic differentiation by signals from blood vessels. Science 2001;294:564–567
16. Kirschner LS, Kusewitt DF, Matyakhina L, et al. A mouse model for the Carney complex tumor syndrome develops neoplasia in cyclic AMP-responsive tissues. Cancer Res 2005;65:4506–4514
17. Song WJ, Schreiber WE, Zhong E, et al. Exendin-4 stimulation of cyclin A2 in beta-cell proliferation. Diabetes 2008;57:2371–2381
18. Hussain MA, Porras DL, Rowe MH, et al. Increased pancreatic beta-cell proliferation mediated by CREB binding protein gene activation. Mol Cell Biol 2006;26:7747–7759
19. Fernandez-Mejia C, Vega-Allende J, Rojas-Ochoa A, et al. Cyclic adenosine 3′,5′-monophosphate increases pancreatic glucokinase activity and gene expression. Endocrinology 2001;142:1448–1452
20. O'Doherty U, Swiggard WJ, Malim MH. Human immunodeficiency virus type 1 spinoculation enhances infection through virus binding. J Virol 2000;74:10074–10080
21. Livak KJ, Schmittgen TD. Analysis of relative gene expression data using real-time quantitative PCR and the 2(-Delta Delta C(T)) Method. Methods 2001;25:402–408
22. Ozaki N, Shibasaki T, Kashima Y, et al. cAMP-GEFII is a direct target of cAMP in regulated exocytosis. Nat Cell Biol 2000;2:805–811
23. de Rooij J, Zwartkruis FJ, Verheijen MH, et al. Epac is a Rap1 guanine-nucleotide-exchange factor directly activated by cyclic AMP. Nature 1998; 396:474–477
24. Kawasaki H, Springett GM, Mochizuki N, et al. A family of cAMP-binding proteins that directly activate Rap1. Science 1998;282:2275–2279
25. Kashima Y, Miki T, Shibasaki T, et al. Critical role of cAMP-GEFII—Rim2 complex in incretin-potentiated insulin secretion. J Biol Chem 2001;276: 46046–46053
26. Kelley GG, Chepurny OG, Schwede F, et al. Glucose-dependent potentiation of mouse islet insulin secretion by Epac activator 8-pCPT-2′-O-Me-cAMP-AM. Islets 2009;1:260–265
27. Dzhura I, Chepurny OG, Leech CA, et al. Phospholipase C-ε links Epac2 activation to the potentiation of glucose-stimulated insulin secretion from mouse islets of Langerhans. Islets 2011;3:121–128
28. Nolan CJ, Madiraju MS, Delghingaro-Augusto V, Peyot ML, Prentki M. Fatty acid signaling in the beta-cell and insulin secretion. Diabetes 2006;55 (Suppl. 2):S16–S23
29. Peyot ML, Pepin E, Lamontagne J, et al. Beta-cell failure in diet-induced obese mice stratified according to body weight gain: secretory dysfunction and altered islet lipid metabolism without steatosis or reduced beta-cell mass. Diabetes 2010;59:2178–2187
30. Araki T, Hirayama M, Hiroi S, Kaku K. GPR40-induced insulin secretion by the novel agonist TAK-875: first clinical findings in patients with type 2 diabetes. Diabetes Obes Metab 2012;14:271–278
31. Ferdaoussi M, Bergeron V, Zarrouki B, et al. G protein-coupled receptor (GPR)40-dependent potentiation of insulin secretion in mouse islets is mediated by protein kinase D1. Diabetologia 2012;55:2682–2692
32. Islam D, Zhang N, Wang P, et al. Epac is involved in cAMP-stimulated proglucagon expression and hormone production but not hormone secretion in pancreatic alpha- and intestinal L-cell lines. Am J Physiol Endocrinol Metab 2009;296:E174–E181
33. Rorsman P, Braun M. Regulation of Insulin Secretion in Human Pancreatic Islets. Annu Rev Physiol 2013;75:155–179
34. Leech CA, Dzhura I, Chepurny OG, Schwede F, Genieser HG, Holz GG. Facilitation of ß-cell K(ATP) channel sulfonylurea sensitivity by a cAMP analog selective for the cAMP-regulated guanine nucleotide exchange factor Epac. Islets 2010;2:72–81
35. Leech CA, Dzhura I, Chepurny OG, et al. Molecular physiology of glucagon-like peptide-1 insulin secretagogue action in pancreatic β cells. Prog Biophys Mol Biol 2011;107:236–247
36. Seino S. Cell signalling in insulin secretion: the molecular targets of ATP, cAMP and sulfonylurea. Diabetologia 2012;55:2096–2108
37. Seino S, Shibasaki T, Minami K. Pancreatic beta-cell signaling: toward better understanding of diabetes and its treatment. Proc Jpn Acad, Ser B, Phys Biol Sci 2010;86:563–577
38. Holz GG 4th, Kühtreiber WM, Habener JF. Pancreatic beta-cells are rendered glucose-competent by the insulinotropic hormone glucagon-like peptide-1(7-37). Nature 1993;361:362–365
39. Kang G, Chepurny OG, Malester B, et al. cAMP sensor Epac as a determinant of ATP-sensitive potassium channel activity in human pancreatic beta cells and rat INS-1 cells. J Physiol 2006;573:595–609
40. Kang G, Leech CA, Chepurny OG, Coetzee WA, Holz GG. Role of the cAMP sensor Epac as a determinant of KATP channel ATP sensitivity in human pancreatic beta-cells and rat INS-1 cells. J Physiol 2008;586:1307–1319
41. Holz GG, Kang G, Harbeck M, Roe MW, Chepurny OG. Cell physiology of cAMP sensor Epac. J Physiol 2006;577:5–15
42. Lemmens R, Larsson O, Berggren PO, Islam MS. Ca2+-induced Ca2+ release from the endoplasmic reticulum amplifies the Ca2+ signal mediated by activation of voltage-gated L-type Ca2+ channels in pancreatic beta-cells. J Biol Chem 2001;276:9971–9977